

Quantum interferometry in multi-mode systems

J. Chwedeńczuk

Faculty of Physics, University of Warsaw, ul. Pasteura 5, PL-02-093 Warszawa, Poland

We consider the situation when the signal propagating through each arm of an interferometer has a complicated multi-mode structure. We find the relation between the particle-entanglement and the possibility to surpass the shot-noise limit of the phase estimation. Our results are general—they apply to pure and mixed states of identical and distinguishable particles (or combinations of both), for a fixed and fluctuating number of particles. We also show that the method for detecting the entanglement often used in two-mode system can give misleading results when applied to the multi-mode case.

I. INTRODUCTION

Interferometers, the most precise metrological instruments constructed by humans, have played a major role in many break-through experiments. In the famous Michelson-Morely failed attempt to detect the ether, the device, now called the “Michelson interferometer”, was used [1]. The negative result of this experiment was relevant for the subsequent formulation of the special theory of relativity. Almost 130 years later, the LIGO team used a similar Michelson setup to detect the gravitational wave coming from a collision of two black holes, which took place over 1 billion years ago [2]. At the moment of the detection, the sensitivity of the LIGO instruments was high enough to observe the displacement ΔL of the test masses $\sim 10^{-22}$ times smaller than the length L of the interferometric arms. With $L \simeq 4$ km, this gives a truly impressive $\Delta L \simeq 10^{-19}$ m, which is $\sim 10^3$ times smaller than the radius of a proton.

Matter-wave interferometers at this moment can measure the gravitational acceleration g with the sensitivity of $\Delta g \simeq 10 \frac{\text{nm}}{\text{s}}$ [3–10]. Once miniaturized, such device could serve as an ultra-precise geological instrument. An atomic interferometer calibrated through the measurement of the close to the surface Casimir-Polder forces could yield information about the gravitational constant G and the possible deviations from the Newton $1/r^2$ scaling of the gravitational force at small distances [11–16]. The gravity-field curvature has recently been observed [17] using an atomic interferometer. Interference of the matter waves is also used in the ultra-precise measurements of the fine-structure constant α , which is of fundamental importance [18–22].

At the current stage, these devices operate at best at the shot-noise level, i.e., the sensitivity of the estimation of the parameter θ does not break the shot-noise limit (SNL), $\Delta\theta \propto \frac{1}{\sqrt{N}}$. Here N is the number of probes—for instance atoms or photons—which carry the information about the interferometric phase. However, theoretical results and multiple proof-of-principle experiments show that the entanglement between these probes is a resource for the sub shot-noise (SSN) sensitivity [23, 24]. Those experiments follow different routes to create non-classical states of light or matter. For instance, the LIGO interferometer already displayed the SSN sensitivity when

one of its input ports was fed with a squeezed state of light [25]. For interferometers operating on matter-waves, the non-classicality is associated with the entanglement between the particles. This effect often manifests through the spin-squeezing of the sample [26–31]. It is a phenomenon—quantified by the spin-squeezing parameter [32, 33]—associated with the two-mode algebra. The use of this algebra is quite natural when discussing the interferometric problems—the two arms are identified with the two modes. Most of the interferometric arguments, such as that relating the entanglement to the SSN sensitivity, are also invoked within this two-mode description. However, in principle, the signal propagating through each arm can have a rich multi-mode structure. This might be a result of thermal excitations, as witnessed in [26], or the inherently multi-mode nature of the process generating the entangled sample, as in [34–38].

Here we generalize the central theorem of quantum metrology—that relating the SSN sensitivity to the entanglement—to the case when each arm of the interferometer has a complicated multi-mode structure [39]. We show that the particle entanglement remains the key resource for beating the SNL. Our proof is of complete generality—it does not make any assumption about the state and works for identical and distinguishable particles or combination of both. Also, it applies to systems with a fixed or fluctuating number of particles. We derive the sensitivity of the phase estimation from the measurement of the population imbalance between the two arms. Finally, we show how the method of detecting the particle entanglement, which works for the two-mode systems, can incorrectly indicate the presence of non-classical correlations in the multi-mode configurations.

This work is organized as follows. In Section II we derive the relation between the entanglement and the SSN sensitivity for identical (Section II A) and distinguishable particles (Section II B). Other configurations are discussed in Section II C. In Section III we calculate the phase sensitivity for the estimation based on the knowledge of the average population imbalance between the two arms. In Section IV we show that the entanglement witness often used for two-mode systems, can give false results in the multi-mode setups. The summary is contained in Section V.

II. ENTANGLEMENT AND SSN SENSITIVITY IN MULTI-MODE SYSTEMS

A. Bosons

1. Multi-mode interferometric transformations

Let a and b denote the two arms of an interferometer. Here, for illustration, we will assume that these arms are spatially separated, however it could be the momentum or other degree of freedom, such as the fine structure, that distinguish a from b . In the standard two-mode case, with each arm a single operator \hat{a} and \hat{b} is associated. The interferometric transformations are generated by the angular-momentum operators

$$\hat{J}_x = \frac{1}{2}(\hat{a}^\dagger \hat{b} + \hat{b}^\dagger \hat{a}), \quad (1a)$$

$$\hat{J}_y = \frac{1}{2i}(\hat{a}^\dagger \hat{b} - \hat{b}^\dagger \hat{a}). \quad (1b)$$

$$\hat{J}_z = \frac{1}{2}(\hat{a}^\dagger \hat{a} - \hat{b}^\dagger \hat{b}). \quad (1c)$$

To account for the multi-mode structure of each arm, we introduce the bosonic field operator $\hat{\Psi}(\mathbf{r})$ which consists of two parts, i.e.,

$$\hat{\Psi}(\mathbf{r}) = \hat{\Psi}_a(\mathbf{r}) + \hat{\Psi}_b(\mathbf{r}). \quad (2)$$

Our aim is to construct the interferometric transformation which will act on the multi-mode arms a and b , rather than on two modes only. It is clear, that such operations can be constructed in many different ways and that the interferometer's performance depends on the structure of the regions as well as on our choice of transformations. To limit the number of possibilities, we will first assume that the mode structure of a and b is the same, and it is only the spatial separation that makes the distinction between them, see Fig. 1. Therefore, each operator can be expanded into its corresponding basis

$$\hat{\Psi}_a(\mathbf{r}) = \sum_n \psi_a^{(n)}(\mathbf{r}) \hat{a}_n, \quad (3a)$$

$$\hat{\Psi}_b(\mathbf{r}) = \sum_n \psi_b^{(n)}(\mathbf{r}) \hat{b}_n, \quad (3b)$$

and the spatial wave-functions are shifted by \mathbf{d} , i.e.,

$$\psi_b^{(n)}(\mathbf{r} + \mathbf{d}) = \psi_a^{(n)}(\mathbf{r}). \quad (4)$$

Also, we assume $|\mathbf{d}|$ to be much larger than the characteristic widths of the wave-packets, giving

$$\psi_a^{(n)}(\mathbf{r}) \psi_b^{(m)}(\mathbf{r}) = 0 \quad \forall n, m. \quad (5)$$

Once the spatial structure of the system is determined, we pick the interferometric transformations. To establish the analogy with the two-mode case, we consider

two types of transformations—the mode mixing and the phase imprint. A natural extension of (1) is

$$\hat{J}_x = \frac{1}{2} \int d\mathbf{r} (\hat{\Psi}_a^\dagger(\mathbf{r}) \hat{\Psi}_b(\mathbf{r} + \mathbf{d}) + \hat{\Psi}_b^\dagger(\mathbf{r} + \mathbf{d}) \hat{\Psi}_a(\mathbf{r})) \quad (6a)$$

$$\hat{J}_y = \frac{1}{2i} \int d\mathbf{r} (\hat{\Psi}_a^\dagger(\mathbf{r}) \hat{\Psi}_b(\mathbf{r} + \mathbf{d}) - \hat{\Psi}_b^\dagger(\mathbf{r} + \mathbf{d}) \hat{\Psi}_a(\mathbf{r})) \quad (6b)$$

$$\hat{J}_z = \frac{1}{2} \int d\mathbf{r} (\hat{\Psi}_a^\dagger(\mathbf{r}) \hat{\Psi}_a(\mathbf{r}) - \hat{\Psi}_b^\dagger(\mathbf{r}) \hat{\Psi}_b(\mathbf{r})). \quad (6c)$$

These integrals can be calculated using relations (4) and (5), and the outcome is

$$\hat{J}_x = \frac{1}{2} \sum_n (\hat{a}_n^\dagger \hat{b}_n + \hat{b}_n^\dagger \hat{a}_n) \equiv \sum_n \hat{J}_x^{(n)} \quad (7a)$$

$$\hat{J}_y = \frac{1}{2i} \sum_n (\hat{a}_n^\dagger \hat{b}_n - \hat{b}_n^\dagger \hat{a}_n) \equiv \sum_n \hat{J}_y^{(n)} \quad (7b)$$

$$\hat{J}_z = \frac{1}{2} \sum_n (\hat{a}_n^\dagger \hat{a}_n - \hat{b}_n^\dagger \hat{b}_n) \equiv \sum_n \hat{J}_z^{(n)}. \quad (7c)$$

Therefore, the mode mixing operators act on each pair of modes separately. This is a result of 1° the assumption about the symmetry between the regions and 2° the particular form of the coupling in Equations (6). While 1° can be regarded as unnatural or highly idealistic, such symmetry is encountered for instance in twin-beam configurations formed by the scattering of atoms from a Bose-Einstein condensate [40]. On the other hand, 2° seems a natural choice: the interferometer should simply “copy” a particle from one arm to another. This second condition can be expressed in other words: the interferometric transformation does not use any knowledge about the internal structure of the arms. It treats each arm as a whole and does not penetrate the inner structure.

The multi-mode interferometric transformations which are single-particle operations (i.e., do not entangle the resources) are usually considered in a form

$$\hat{U}(\theta) = e^{-i\theta \hat{J}_n}. \quad (8)$$

Here $\hat{J}_n = \vec{n} \cdot \hat{\mathbf{J}}$ is a scalar product of a unit vector \vec{n} and a vector of the angular momentum operators [41]. We will now demonstrate that, in analogy to the two-mode case, the particle entanglement is a necessary resource for beating the shot-noise limit of the phase estimation also in the multi-mode case.

2. Role of the particle entanglement

Let us begin with a two-mode separable (i.e., non-entangled) pure state of N bosons. It is the spin-coherent state

$$|z, \varphi; N\rangle = \frac{1}{\sqrt{N!}} \left(\sqrt{z} e^{i\varphi} \hat{a}^\dagger + \sqrt{1-z} \hat{b}^\dagger \right)^N |0\rangle. \quad (9)$$

Here, $z \in [0, 1]$ is the population imbalance between the two modes, while $\varphi \in [0, 2\pi]$ is the relative phase. This

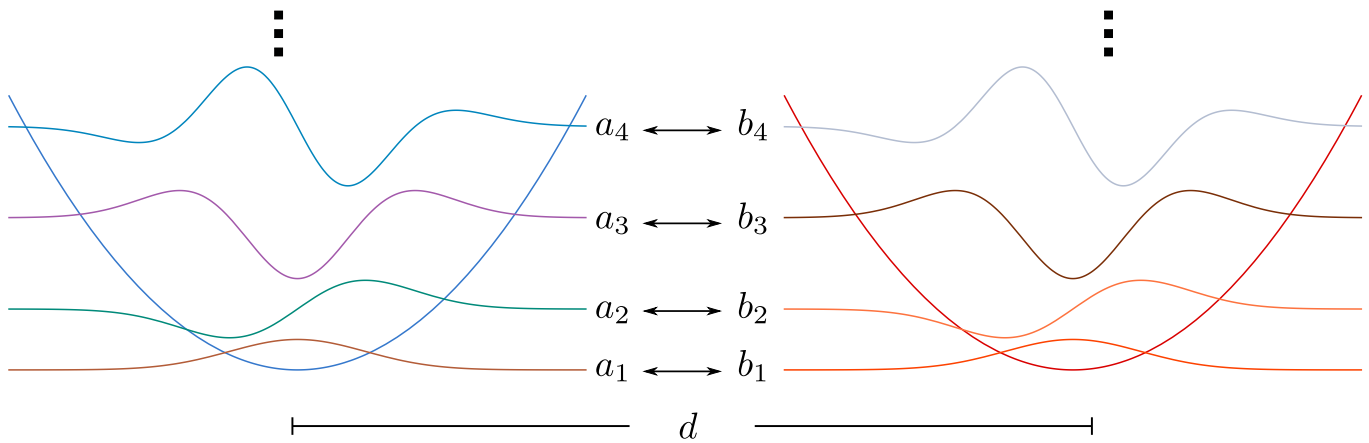


FIG. 1. The two-arm, multi-mode interferometer, illustrated here with the eigen-modes of the harmonic oscillator. Each arm (here a harmonic well) has the same ladder of states, just shifted by d . The interferometric transformation can either imprint the relative phase between the arms or move the particles from one arm to the other.

state is a basic building block of the density matrix of N non-entangled bosons, which reads

$$\hat{\rho}_{\text{sep}} = \int_0^1 dz \int_0^{2\pi} d\varphi \mathcal{P}(z, \varphi) |z, \varphi; N\rangle \langle z, \varphi; N|, \quad (10)$$

where \mathcal{P} is a probability distribution of the variables (z, φ) . The expression (10) is the fixed- N analog of the classical state of the electromagnetic field, according to the Glauber-Sudarshan criterion [42–45]. The expressions (9) and (10) can be easily generalized to the multi-mode setup. Namely, the former transforms to

$$|z, \varphi; N\rangle \rightarrow |\vec{\alpha}, \vec{\beta}; N\rangle = \frac{1}{\sqrt{N!}} \left(\vec{\alpha} \hat{a}^\dagger + \vec{\beta} \hat{b}^\dagger \right)^N |0\rangle. \quad (11)$$

The vectors of complex amplitudes $\vec{\alpha}$ and $\vec{\beta}$ are normalized, i.e. $|\vec{\alpha}|^2 + |\vec{\beta}|^2 = 1$, while \hat{a} and \hat{b} are vectors of mode operators introduced in Eq. (3). Similarly, the density matrix of unentangled bosons now reads [46]

$$\hat{\rho}_{\text{sep}} = \iint d\vec{\alpha} d\vec{\beta} \mathcal{P}(\vec{\alpha}, \vec{\beta}) |\vec{\alpha}, \vec{\beta}; N\rangle \langle \vec{\alpha}, \vec{\beta}; N|. \quad (12)$$

We will show that for the separable states (12) and the interferometric transformations (8), the phase estimation sensitivity is bounded by the shot-noise.

The sensitivity of the phase estimation is limited by the Cramer-Rao lower bound [47]

$$\Delta\theta \geq \frac{1}{\sqrt{m}} \frac{1}{\sqrt{F_q}}. \quad (13)$$

Here, m is the number of the independent repetitions of the estimation experiment. The F_q is called the quantum Fisher information (QFI) and it quantifies the amount of information about θ , which can be extracted from m measurements using any estimation strategy [48]. For pure states, the QFI is simple to calculate,

$$F_q = 4(\langle \hat{J}_n^2 \rangle - \langle \hat{J}_n \rangle^2) \equiv 4\langle (\Delta \hat{J}_n)^2 \rangle, \quad (14)$$

where the mean is calculated with the state undergoing the interferometric transformation. For mixed states, the QFI is much more complex,

$$F_q = 2 \sum_{i,j} \frac{(p_i - p_j)^2}{p_i + p_j} \left| \langle i | \hat{J}_n | j \rangle \right|^2, \quad (15)$$

where $|i/j\rangle$ are the eigen-vectors and $p_{i/j}$ are the corresponding eigen-values of the density matrix. Therefore, to obtain the F_q , one would need to diagonalize $\hat{\rho}_{\text{sep}}$ from Eq. (12), which is numerically feasible, but analytically very hard, since different $|\vec{\alpha}, \vec{\beta}; N\rangle$'s are not orthogonal, just as nonorthogonal are the coherent states of light. However, a useful feature of the QFI—its convexity—allows to lower-bound the sensitivity for mixed states. Namely, for $\hat{\rho} = \sum_i p_i \hat{\rho}_i$, i.e., a statistical mixture of density matrices, we have

$$F_q \left[\sum_i p_i \hat{\rho}_i \right] \leq \sum_i p_i F_q[\hat{\rho}_i]. \quad (16)$$

This property, applied to Eq. (12), gives

$$F_q \leq \iint d\vec{\alpha} d\vec{\beta} \mathcal{P}(\vec{\alpha}, \vec{\beta}) F_q^{(\vec{\alpha}, \vec{\beta})}. \quad (17)$$

Here, $F_q^{(\vec{\alpha}, \vec{\beta})}$ is the QFI calculated with a pure state $|\vec{\alpha}, \vec{\beta}; N\rangle$, thus it is given by Eq. (14).

We calculate the QFI for $\hat{J}_{\vec{n}} = \hat{J}_z$ and show that for separable states, $F_q \leq N$. Any other direction \vec{n}' can be obtained by a series of rotations of \hat{J}_z , generated by the operators (7). They are single-particle objects, therefore, once applied to the separable state (12), rather than to the evolution operator, they would transform one $\hat{\rho}_{\text{sep}}$ into another, i.e., would only change $\mathcal{P}(\vec{\alpha}, \vec{\beta})$ into some $\tilde{\mathcal{P}}(\vec{\alpha}, \vec{\beta})$, but will not modify the structure of Eq. (12). Thus it is enough to show that $F_q \leq N$ for \hat{J}_z and a general probability distribution.

First, we calculate $F_q^{(\vec{\alpha}, \vec{\beta})}$ with Eq. (14). The mean of \hat{J}_z is

$$\langle \hat{J}_z \rangle = \frac{N}{2} \sum_n (|\alpha_n|^2 - |\beta_n|^2) \equiv \frac{N}{2} (|\vec{\alpha}|^2 - |\vec{\beta}|^2), \quad (18)$$

where we used the expression (6c) and the relation

$$\hat{a}_n |\vec{\alpha}, \vec{\beta}; N\rangle = \sqrt{N} \alpha_n |\vec{\alpha}, \vec{\beta}; N-1\rangle, \quad (19a)$$

$$\hat{b}_n |\vec{\alpha}, \vec{\beta}; N\rangle = \sqrt{N} \beta_n |\vec{\alpha}, \vec{\beta}; N-1\rangle. \quad (19b)$$

The second moment is calculated in a similar way, i.e.,

$$\langle \hat{J}_z^2 \rangle = \sum_{n,m} \langle \hat{J}_z^{(n)} \hat{J}_z^{(m)} \rangle = \sum_n \langle (\hat{J}_z^{(n)})^2 \rangle + \sum_{n \neq m} \langle \hat{J}_z^{(n)} \hat{J}_z^{(m)} \rangle. \quad (20)$$

The two contributions must be treated separately

$$\begin{aligned} \sum_n \langle (\hat{J}_z^{(n)})^2 \rangle &= \frac{N}{4} \left[1 + (N-1) \sum_n (|\alpha_n|^2 - |\beta_n|^2)^2 \right], \\ \sum_{n \neq m} \langle \hat{J}_z^{(n)} \hat{J}_z^{(m)} \rangle &= \frac{N(N-1)}{4} \times \\ &\quad \times \sum_{n \neq m} (|\alpha_n|^2 - |\beta_n|^2) (|\alpha_m|^2 - |\beta_m|^2). \end{aligned}$$

We add these two terms and obtain

$$\langle \hat{J}_z^2 \rangle = \frac{N}{4} + \frac{N(N-1)}{4} (|\vec{\alpha}|^2 - |\vec{\beta}|^2)^2. \quad (21)$$

The subtraction of the squared mean from Eq. (18) gives

$$0 \leq F_q^{(\vec{\alpha}, \vec{\beta})} = N \left(1 - (|\vec{\alpha}|^2 - |\vec{\beta}|^2)^2 \right) \leq N. \quad (22)$$

This result, combined with Eq. (17) yields

$$F_q \leq N. \quad (23)$$

Since the QFI can surpass the SNL, for instance with two-mode spin-squeezed states, we conclude that the particle entanglement is the resource for the SSN metrology also in multi-mode systems. We now extend the above formalism to distinguishable particles.

B. Distinguishable particles

1. Multi-mode interferometric transformations

Note that the formalism of second quantization allows for a quick generalization of the above results to distinguishable particles. Namely, another index must be attributed to the operators \hat{a}_n and \hat{b}_n , such that labels the species of the particle (and of the associated field). This way, for the particle of type j , we obtain $\hat{a}_n^{(j)}$ and $\hat{b}_n^{(j)}$. The interferometric transformations cannot transmute a particle of one type into another—such process would violate the conservation laws and the related super-selection rules [46, 49, 50]. Thus a particle of each type undergoes a separate transformation, which means that the operators (6) change into

$$\hat{J}_x = \frac{1}{2} \sum_{j=1}^N \sum_n \left(\hat{a}_n^{(j)\dagger} \hat{b}_n^{(j)} + \hat{b}_n^{(j)\dagger} \hat{a}_n^{(j)} \right) \quad (24a)$$

$$\hat{J}_y = \frac{1}{2i} \sum_{j=1}^N \sum_n \left(\hat{a}_n^{(j)\dagger} \hat{b}_n^{(j)} - \hat{b}_n^{(j)\dagger} \hat{a}_n^{(j)} \right) \quad (24b)$$

$$\hat{J}_z = \frac{1}{2} \sum_{j=1}^N \sum_n \left(\hat{a}_n^{(j)\dagger} \hat{a}_n^{(j)} - \hat{b}_n^{(j)\dagger} \hat{b}_n^{(j)} \right). \quad (24c)$$

Once the interferometric transformations are determined, we discuss the role of the particle entanglement for the SSN sensitivity.

2. Role of the particle entanglement

The separable state of N distinguishable particles is constructed from the one-body pure states. For the particle of type j distributed among a and b it reads

$$|\vec{\alpha}^{(j)}, \vec{\beta}^{(j)}; N\rangle = \left(\vec{\alpha}^{(j)} \hat{a}^{(j)\dagger} + \vec{\beta}^{(j)} \hat{b}^{(j)\dagger} \right) |0\rangle. \quad (25)$$

The parallel with the coherent state from Eq. (11) is evident and it is even more pronounced when the separable state of distinguishable particles is introduced

$$\hat{\rho}_{\text{sep}} = \iint d\vec{\alpha}^{(1)} d\vec{\beta}^{(1)} \dots \iint d\vec{\alpha}^{(N)} d\vec{\beta}^{(N)} \mathcal{P}(\vec{\alpha}^{(1)}, \vec{\beta}^{(1)}, \dots, \vec{\alpha}^{(N)}, \vec{\beta}^{(N)}) \bigotimes_{i=1}^N |\vec{\alpha}^{(i)}, \vec{\beta}^{(i)}; N\rangle \langle \vec{\alpha}^{(i)}, \vec{\beta}^{(i)}; N|. \quad (26)$$

The state of N distinguishable and non-entangled particles is the state (12) but with each mode—now labeled with two numbers n and j , rather than with n only—occupied with one particle. The deep analogy holds since the transformation (24) cannot transmute the particles.

Once this close relation is noticed, the QFI can be bounded from above in a similar fashion to that presented in Section II A 2 and the calculation is straightforward. We again pick the interferometric transformation to be generated by \hat{J}_z and using the convexity of the QFI declared in Eq. (17), we have

$$F_q \leq \iint d\vec{\alpha}^{(1)} d\vec{\beta}^{(1)} \dots \iint d\vec{\alpha}^{(N)} d\vec{\beta}^{(N)} \mathcal{P}(\vec{\alpha}^{(1)}, \vec{\beta}^{(1)}, \dots, \vec{\alpha}^{(N)}, \vec{\beta}^{(N)}) \sum_{j=1}^N F_q^{(\vec{\alpha}^{(j)}, \vec{\beta}^{(j)})}. \quad (27)$$

Here we used the fact that the operator (24c) acts on each particle independently. Every $F_q^{(\vec{\alpha}^{(j)}, \vec{\beta}^{(j)})}$ is calculated with a single-particle state (25), therefore it is bounded as in Eq. (22) but with $N = 1$ (because there is only a single particle of a given type), namely

$$0 \leq F_q^{(\vec{\alpha}^{(j)}, \vec{\beta}^{(j)})} = \left[1 - (|\vec{\alpha}^{(j)}|^2 - |\vec{\beta}^{(j)}|^2)^2 \right] \leq 1. \quad (28)$$

Therefore the sum from Eq. (27) is bounded as follows

$$\sum_{j=1}^N F_q^{(\vec{\alpha}^{(j)}, \vec{\beta}^{(j)})} \leq N. \quad (29)$$

Since \mathcal{P} from Eq. (27) is normalized we obtain

$$F_q \leq N \quad (30)$$

for all separable states of distinguishable particles defined in Eq. (26). On the other hand, take an entangled NOON state of N distinguishable particles—for instance each in the same spatial mode—in the form

$$|\psi\rangle = \frac{1}{\sqrt{2}} \left(\prod_{j=1}^N \hat{a}^{(j)\dagger} + \prod_{j=1}^N \hat{b}^{(j)\dagger} \right) |0\rangle. \quad (31)$$

This state will give $F_q = N^2$ (the Heisenberg scaling), therefore the QFI is a witness of particle entanglement also for distinguishable particles.

C. Other cases

For the story to be complete we must consider two other possible cases. One is when the system contains both distinguishable particles and bosons, all together forming a separable state. Again, we repeat that the interferometric transformations—to be consistent with the conservation laws and the super-selection rules—cannot transmute the particles from these two groups into each other. Therefore, since they form a separable state where the mode occupied by each particle can be addressed individually, the set of distinguishable particles and bosons can be treated separately. Thus to each of these sets the arguments from the above sections apply, so also in such configuration the particle-entanglement will be a necessary resource to beat the shot-noise limit.

Another possibility is that the system does not contain a fixed number of particles, but rather its amount fluctuates from shot to shot, governed by the probability distribution $P(N)$. The separable state is now

$$\hat{\rho}_{\text{sep}} = \sum_{N=0}^{\infty} P(N) \hat{\rho}_{\text{sep}}^{(N)}, \quad (32)$$

where $\hat{\rho}_{\text{sep}}^{(N)}$ contains N particles and is given either by Eq. (12) or (26) or by a mixture of those, as discussed in the above paragraph. Since the operators \hat{J}_i do not couple states with different number of particles, each fixed- N sector can be treated separately. Therefore, using again the convexity of the QFI, in all the cases we obtain for separable states

$$F_q \leq \sum_{N=0}^{\infty} P(N) N \equiv \langle N \rangle, \quad (33)$$

which defines the shot-noise limit [51].

Finally, we note that these arguments do not apply to collections of fermions, for which the separable states do not exist due to the Pauli exclusion principle.

III. ESTIMATION FROM THE MEAN POPULATION IMBALANCE

We now abandon the general considerations and switch to a particular phase estimation protocol. We derive the phase sensitivity for a multi-mode Mach-Zehnder interferometer (MZI). We take the most common estimation protocol, where the phase is deduced from the average population imbalance between the two regions. Although the derivation is done for bosons, according to the above arguments the results apply also to distinguishable particles and collections of both.

In analogy to the two-mode case, the multi-mode MZI evolution operator is

$$\hat{U}(\theta) = e^{-i\theta \hat{J}_y}, \quad (34)$$

with the generator given by Eq. (7b). At the output, in the i -th repetition of the experiment, the number of particles in each arm is measured, i.e., $n_a^{(i)}$ and $n_b^{(i)}$. From this data, the population imbalance between the two subsystems is calculated, $n_i = \frac{n_a^{(i)} - n_b^{(i)}}{2}$, and the sequence is repeated m times and averaged to give

$$\bar{n}_m = \frac{1}{m} \sum_{i=1}^m n_i. \quad (35)$$

If $m \gg 1$, the central limit theorem tells that the probability for obtaining \bar{n}_m is a Gaussian function

$$p(\bar{n}_m) \propto \exp \left[-m \frac{\left(\bar{n}_m - \langle \hat{J}_z(\theta) \rangle \right)^2}{2 \langle (\Delta \hat{J}_z(\theta))^2 \rangle} \right]. \quad (36)$$

When the phase is estimated from the maximum of the likelihood function for this probability, we obtain

$$\Delta^2\theta = \frac{1}{m} \frac{\langle(\Delta\hat{J}_z(\theta))^2\rangle}{\left(\frac{\partial\langle\hat{J}_z(\theta)\rangle}{\partial\theta}\right)^2}. \quad (37)$$

The $\hat{J}_z(\theta)$ is obtained by evolving the \hat{J}_z with the operator (34), i.e.,

$$\hat{J}_z(\theta) = \hat{U}^\dagger(\theta)\hat{J}_z\hat{U}(\theta) = \hat{J}_z \cos\theta + \hat{J}_x \sin\theta, \quad (38)$$

where the last equality was obtained using the commutation relations of operators (6) and the Baker–Campbell–Hausdorff formula. Substitution of the result (38) into Eq. (37) gives for $\theta = 0$

$$\Delta^2\theta = \frac{1}{m} \frac{\langle(\Delta\hat{J}_z)^2\rangle}{\langle\hat{J}_x\rangle^2}. \quad (39)$$

This is a natural extension of the spin-squeezing parameter (for balanced systems, where $\langle\hat{J}_y\rangle = 0$), to the multi-mode case. The combination of Equations (13) and (23) means that also

$$\xi^2 = N \frac{\langle(\Delta\hat{J}_z)^2\rangle}{\langle\hat{J}_x\rangle^2} \quad (40)$$

is a witness of quantum correlations among the particles—when $\xi^2 < 1$ the system is particle-entangled. We now show that the measurement of this quantity in the multi-mode system is not as straightforward as in the two-mode case.

IV. DETECTION OF ENTANGLEMENT—FLUCTUATIONS AND VISIBILITY

First however we recall that for the two-mode systems, the spin-squeezing parameter is defined as

$$\xi_S^2 = N \frac{\langle(\Delta\hat{J}_3)^2\rangle}{\langle\hat{J}_1\rangle^2 + \langle\hat{J}_2\rangle^2}. \quad (41)$$

Here 1, 2, 3 are three orthogonal directions obtained by the combinations of \hat{J}_x , \hat{J}_y and \hat{J}_z from Equations (6). When $\xi_S^2 < 1$, the system is spin-squeezed—it is particle-entangled and useful for quantum metrology [23]. It is most common to take (1, 2, 3) as (x, y, z) , giving

$$\xi_S^2 = N \frac{\langle(\Delta\hat{J}_z)^2\rangle}{\langle\hat{J}_x\rangle^2 + \langle\hat{J}_y\rangle^2}. \quad (42)$$

The motivation for this particular choice lies in direct experimental accessibility both to the nominator and the denominator of Eq. (42). This can be particularly easily seen when the average number of atoms in each mode is

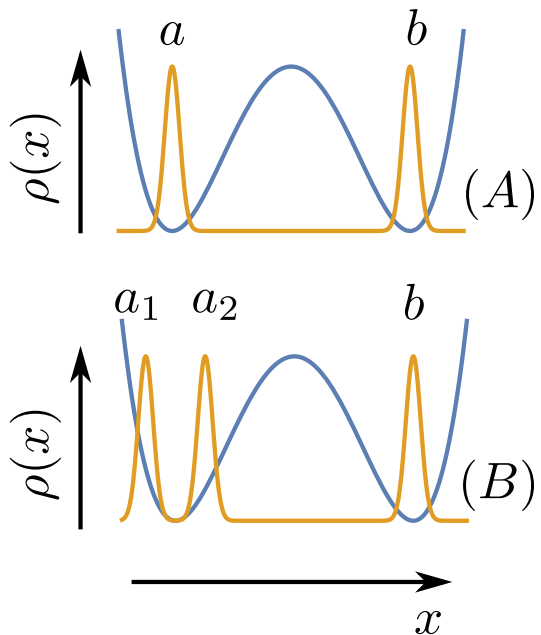


FIG. 2. The single-particle density of atoms trapped in a double-well potential. (A) The standard two-mode setup. (B) The three-mode setup: the configuration after a coherent splitting of the a mode into a_1 and a_2 .

high. In this case, the mode operators can be approximated as follows

$$\hat{a} \simeq \sqrt{n_a} e^{i\frac{\phi}{2}}, \quad \hat{b} \simeq \sqrt{n_b} e^{-i\frac{\phi}{2}}. \quad (43)$$

Here, $n_{a/b}$ are the average mode occupations and ϕ is the relative phase, which fluctuates from shot to shot. In this approximation, the average of \hat{J}_x and \hat{J}_y is

$$\langle\hat{J}_x\rangle = \sqrt{n_a n_b} \langle\cos\phi\rangle, \quad \langle\hat{J}_y\rangle = \sqrt{n_a n_b} \langle\sin\phi\rangle. \quad (44)$$

Similarly, the atom number fluctuations normalized to the shot-noise is

$$\xi_N^2 = N \frac{\langle(\Delta\hat{J}_z)^2\rangle}{n_a n_b}. \quad (45)$$

Therefore, the spin squeezing from Eq. (42) can be expressed as follows

$$\xi_S^2 = \frac{\xi_N^2}{\langle\cos\phi\rangle^2 + \langle\sin\phi\rangle^2}. \quad (46)$$

Note that for the spin-coherent state $\xi_N^2 \equiv 1$, while the phase is fixed and does not fluctuate from shot to shot, so that $\langle\cos\phi\rangle^2 + \langle\sin\phi\rangle^2 = \cos^2\phi + \sin^2\phi = 1$, giving $\xi_S^2 = 1$: the system is not spin-squeezed. In the experiments, the atom number fluctuations are calculated by measuring in each shot the population of each mode. In another series of experiments, the two modes are let interfere and the relative phase of the pattern is recorded to give, after many runs, the denominator of Eq. (46).

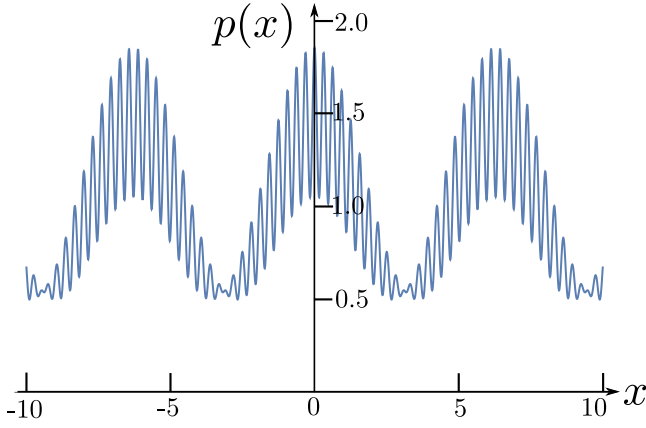


FIG. 3. The single-particle far-field interference pattern, see Eq. (54), formed by a coherent spin-state (52) in the three-mode configuration shown in Fig. 2(B). The parameters are $z = 0.91$, $\zeta = 0.5$, $k = 10$ and $\delta k = 0.5$.

Note that there is an alternative method for measuring (42), which does not rely on the mean-field approximation (43). In the far-field, the spatial wave-packet of the modes a and b are plane-waves (or, more precisely broad functions with fast oscillations on top), i.e.,

$$\hat{\Psi}(x) = e^{ikx} \hat{a} + e^{-ikx} \hat{b}. \quad (47)$$

The density of this system is

$$\rho(x) = \langle \hat{\Psi}^\dagger(x) \hat{\Psi}(x) \rangle = \langle \hat{a}^\dagger \hat{a} \rangle + \langle \hat{b}^\dagger \hat{b} \rangle + 2\langle \hat{J}_x \rangle \cos(2kx) + 2\langle \hat{J}_y \rangle \sin(2kx). \quad (48)$$

Since $\langle \hat{a}^\dagger \hat{a} \rangle + \langle \hat{b}^\dagger \hat{b} \rangle = N$, the normalized density reads

$$\begin{aligned} p(x) &= \frac{1}{N} \rho(x) = 1 + \nu_1 \cos(2kx) + \nu_2 \sin(2kx) = \\ &= 1 + \nu \cos(2kx - \alpha), \end{aligned} \quad (49)$$

where $\nu_{1/2} = \frac{2}{N} \langle \hat{J}_{x/y} \rangle$ and $\alpha = \arccos(\frac{\nu_1}{\nu})$, while $\nu = \sqrt{\nu_1^2 + \nu_2^2}$ is the fringe visibility. Therefore, the spin-squeezing (42) can be expressed in terms of the atom

$$p(x) = \frac{1}{N} \langle \hat{\Psi}^\dagger(x) \hat{\Psi}(x) \rangle = 1 + z \sqrt{\zeta(1-\zeta)} \cos(2\delta kx) + \sqrt{z(1-z)} \left(\sqrt{\zeta} \cos((2k + \delta k)x) + \sqrt{1-\zeta} \cos((2k - \delta k)x) \right). \quad (54)$$

This density is plotted in Fig. (3) with $z = 0.91$, $\zeta = 0.5$, $k = 10$ and $\delta k = 0.5$. The fringe visibility, calculated as the ratio $\nu = (p_{\max} - p_{\min}) / (p_{\max} + p_{\min})$ is $\nu^2 = 0.326$. This combined with the normalized population imbalance between the two regions, $\eta^2 = 1 - (2z - 1)^2 = 0.321$, gives the ratio $\eta^2 / \nu^2 = 0.988$, suggesting the presence of the particle entanglement in the system. However, it is a false statement: ν cannot be identified with the denominator of Eq. (40) in this case.

number fluctuations $\eta^2 = \frac{4}{N} \langle (\Delta \hat{J}_z)^2 \rangle$ and the visibility

$$\xi_S^2 = \frac{\eta^2}{\nu^2}. \quad (50)$$

We now demonstrate that the use of this operational definition of the spin-squeezing, without the *a priori* knowledge about the mode structure of each arm, can lead to false conclusions regarding the presence of the particle entanglement in the system.

In the multi-mode case, the density calculated with the operator (2) is

$$\rho(x) = \rho_{aa}(x) + \rho_{bb}(x) + \rho_{ab}(x) + \rho_{ba}(x), \quad (51)$$

where $\rho_{ij}(x) = \langle \hat{\Psi}_i^\dagger(x) \hat{\Psi}_j^\dagger(x) \rangle$. Clearly the density contains multiple interference terms, not only resulting from the overlap of the wave-functions coming from the opposite regions but also from different modes residing initially in the same region. Therefore, the visibility of fringes cannot be linked to the denominator of Eq. (40), which only quantifies the a/b coherence. For illustration, take a coherent spin state from Eq. (9) with $\varphi = 0$. Assume now that in the region a , some process splits the mode a into the coherent superposition of a_1 and a_2 , schematically shown in Fig. 2 in a double-well setup. This way, a state

$$|\psi\rangle = \frac{1}{\sqrt{N!}} \left[\sqrt{z} \left(\sqrt{\zeta} \hat{a}_1^\dagger + \sqrt{1-\zeta} \hat{a}_2^\dagger \right) + \sqrt{1-z} \hat{b}_1^\dagger \right]^N |0\rangle \quad (52)$$

is obtained. It is an example of a non-entangled state from Eq. (11) with $\vec{\alpha} = \sqrt{z}(\sqrt{\zeta}, \sqrt{1-\zeta}, 0 \dots)^T$ and $\vec{\beta} = (\sqrt{1-z}, 0 \dots)^T$. The splitting does not influence the nominator of Eq. (40), but in the far-field the interference of the two modes a_1 and a_2 will have impact on the visibility of fringes. The field operator after the expansion will read

$$\hat{\Psi}(x) = e^{i(k+\delta k)x} \hat{a}_1 + e^{i(k-\delta k)x} \hat{a}_2 + e^{-ikx} \hat{b}. \quad (53)$$

giving the normalized density

Some remarks—Naturally, the three-mode example invoked here is quite artificial. It is hard to imagine that a coherent physical process, which splits \hat{a} into \hat{a}_1 and \hat{a}_2 could be uncontrolled and unnoticed by the experimentalists. Also, any experimentalist would immediately notice two frequencies of oscillations in the interference pattern. Last but not least, usually the multi-mode structure of the two regions a and b comes from the thermal excitations, and thus reveals no coherence between

the modes. Nevertheless, the example shows that the method of detecting the particle-entanglement through the fluctuations-to-visibility ratio can be safely used only when the structure of each sub-system is known.

V. SUMMARY

The main outcome of this work is the establishment of the SNL for the two-arm multi-mode interferometers. This is a general result, as it applies to any thinkable quantum system where the entangled/non-entangled dichotomy exists. It is valid for both fixed- and non-fixed- N systems, for as long as the coherence between states carrying different number of particles is absent.

Note that our results are valid for a particular choice of the interferometric transformations, such that do not penetrate the inner structure of each arm but rather treat them as a whole. In principle, any other type of such transformation requires a dedicated calculation of the SNL. Otherwise, conclusions about the presence of metrologically useful particle entanglement in the system can be incorrect.

We have also calculated the phase sensitivity for the standard estimation protocol based on the knowledge of the mean population imbalance between the two arms. Finally, we have shown that if the popular method of detecting the entanglement in two-mode systems is used without the *a priori* knowledge about the modal structure of the arms, a false conclusion from the number-fluctuations-to-visibility ratio can be drawn.

-
- [1] R. A. Schumacher, American Journal of Physics **62**, 609 (1994).
- [2] B. P. Abbott *et al.*, Physical Review Letters **116**, 061102 (2016).
- [3] K. S. Hardman, P. J. Everitt, G. D. McDonald, P. Manju, P. B. Wigley, M. A. Sooriyabandara, C. C. N. Kuhn, J. E. Debs, J. D. Close, and N. P. Robins, Phys. Rev. Lett. **117**, 138501 (2016).
- [4] G. Ferrari, N. Poli, F. Sorrentino, and G. M. Tino, Phys. Rev. Lett. **97**, 060402 (2006).
- [5] N. Poli, F.-Y. Wang, M. G. Tarallo, A. Alberti, M. Prevedelli, and G. M. Tino, Phys. Rev. Lett. **106**, 038501 (2011).
- [6] M. J. Snadden, J. M. McGuirk, P. Bouyer, K. G. Haritos, and M. A. Kasevich, Phys. Rev. Lett. **81**, 971 (1998).
- [7] J. M. McGuirk, M. J. Snadden, and M. A. Kasevich, Phys. Rev. Lett. **85**, 4498 (2000).
- [8] J. M. McGuirk, G. T. Foster, J. B. Fixler, M. J. Snadden, and M. A. Kasevich, Phys. Rev. A **65**, 033608 (2002).
- [9] N. Poli, F.-Y. Wang, M. G. Tarallo, A. Alberti, M. Prevedelli, and G. M. Tino, Phys. Rev. Lett. **106**, 038501 (2011).
- [10] M. Andia, R. Jannin, F. m. c. Nez, F. m. c. Biraben, S. Guellati-Khélifa, and P. Cladé, Phys. Rev. A **88**, 031605 (2013).
- [11] M. Antezza, L. P. Pitaevskii, and S. Stringari, Phys. Rev. A **70**, 053619 (2004).
- [12] I. Carusotto, L. Pitaevskii, S. Stringari, G. Modugno, and M. Inguscio, Phys. Rev. Lett. **95**, 093202 (2005).
- [13] D. M. Harber, J. M. Obrecht, J. M. McGuirk, and E. A. Cornell, Phys. Rev. A **72**, 033610 (2005).
- [14] J. M. Obrecht, R. J. Wild, M. Antezza, L. P. Pitaevskii, S. Stringari, and E. A. Cornell, Phys. Rev. Lett. **98**, 063201 (2007).
- [15] J. Chwedeńczuk, L. Pezzé, F. Piazza, and A. Smerzi, Phys. Rev. A **82**, 032104 (2010).
- [16] G. Lamporesi, A. Bertoldi, L. Cacciapuoti, M. Prevedelli, and G. M. Tino, Phys. Rev. Lett. **100**, 050801 (2008).
- [17] G. Rosi, L. Cacciapuoti, F. Sorrentino, M. Menchetti, M. Prevedelli, and G. M. Tino, Phys. Rev. Lett. **114**, 013001 (2015).
- [18] P. Cladé, E. de Mirandes, M. Cadoret, S. Guellati-Khélifa, C. Schwob, F. m. c. Nez, L. Julien, and F. m. c. Biraben, Phys. Rev. A **74**, 052109 (2006).
- [19] R. Bouchendira, P. Cladé, S. Guellati-Khélifa, F. m. c. Nez, and F. m. c. Biraben, Phys. Rev. Lett. **106**, 080801 (2011).
- [20] P. Cladé, E. de Mirandes, M. Cadoret, S. Guellati-Khélifa, C. Schwob, F. m. c. Nez, L. Julien, and F. m. c. Biraben, Phys. Rev. Lett. **96**, 033001 (2006).
- [21] R. Battesti, P. Cladé, S. Guellati-Khélifa, C. Schwob, B. Grémaud, F. m. c. Nez, L. Julien, and F. m. c. Biraben, Phys. Rev. Lett. **92**, 253001 (2004).
- [22] M. Cadoret, E. de Mirandes, P. Cladé, S. Guellati-Khélifa, C. Schwob, F. m. c. Nez, L. Julien, and F. m. c. Biraben, Phys. Rev. Lett. **101**, 230801 (2008).
- [23] V. Giovannetti, S. Lloyd, and L. Maccone, Science **306**, 1330 (2004).
- [24] L. Pezzé and A. Smerzi, Phys. Rev. Lett. **102**, 100401 (2009).
- [25] LIGO Scientific Collaboration, Nat. Phys. **7**, 962 (2011).
- [26] J. Esteve, C. Gross, A. Weller, S. Giovanazzi, and M. Oberthaler, Nature **455**, 1216 (2008).
- [27] T. Berrada, S. van Frank, R. Bücker, T. Schumm, J.-F. Schaff, and J. Schmiedmayer, Nat. Commun. **4** (2013).
- [28] I. D. Leroux, M. H. Schleier-Smith, and V. Vuletić, Phys. Rev. Lett. **104**, 250801 (2010).
- [29] Z. Chen, J. G. Bohnet, S. R. Sankar, J. Dai, and J. K. Thompson, Phys. Rev. Lett. **106**, 133601 (2011).
- [30] C. Gross, T. Zibold, E. Nicklas, J. Esteve, and M. K. Oberthaler, Nature **464**, 1165 (2010).
- [31] J. Appel, P. J. Windpassinger, D. Oblak, U. B. Hoff, N. Kjærgaard, and E. S. Polzik, PNAS **106**, 10960 (2009).
- [32] M. Kitagawa and M. Ueda, Phys. Rev. A **47**, 5138 (1993).
- [33] D. Wineland, J. Bollinger, W. Itano, and D. Heinzen, Phys. Rev. A **50**, 67 (1994).
- [34] B. Lücke, M. Scherer, J. Kruse, L. Pezzé, F. Deuretzbacher, P. Hyllus, J. Peise, W. Ertmer, J. Arlt, L. Santos, *et al.*, Science **334**, 773 (2011).
- [35] R. Bücker, J. Grund, S. Manz, T. Berrada, T. Betz, C. Koller, U. Hohenester, T. Schumm, A. Perrin, and J. Schmiedmayer, Nat. Phys. **7**, 608 (2011).
- [36] K. V. Kheruntsyan, J.-C. Jaskula, P. Deuar, M. Bonneau,

- G. B. Partridge, J. Ruaudel, R. Lopes, D. Boiron, and C. I. Westbrook, Phys. Rev. Lett. **108**, 260401 (2012).
- [37] A. Perrin, H. Chang, V. Krachmalnicoff, M. Schellekens, D. Boiron, A. Aspect, and C. I. Westbrook, Phys. Rev. Lett. **99**, 150405 (2007).
- [38] W. RuGway, S. S. Hodgman, R. G. Dall, M. T. Johnsson, and A. G. Truscott, Phys. Rev. Lett. **107**, 075301 (2011).
- [39] E. Andersson, T. Calarco, R. Folman, M. Andersson, B. Hessmo, and J. Schmiedmayer, Phys. Rev. Lett. **88**, 100401 (2002).
- [40] T. Wasak, P. Szańkowski, R. Bücker, J. Chwedeńczuk, and M. Trippenbach, New Journal of Physics **16**, 013041 (2014).
- [41] Note that in principle, an interferometer can be a series of linear transformations, rather than a single one [52]. Still, such composite operation remains linear and does not entangle the particles.
- [42] R. J. Glauber, Phys. Rev. **131**, 2766 (1963).
- [43] E. C. G. Sudarshan, Phys. Rev. Lett. **10**, 277 (1963).
- [44] T. Wasak, P. Szańkowski, P. Ziń, M. Trippenbach, and J. Chwedeńczuk, Phys. Rev. A **90**, 033616 (2014).
- [45] T. Wasak, P. Szańkowski, M. Trippenbach, and J. Chwedeńczuk, Quantum Information Processing **15**, 269 (2015).
- [46] T. Wasak, A. Smerzi, and J. Chwedeńczuk, arXiv:1609.01576 (2016).
- [47] A. Holevo, *Probabilistic and Statistical Aspects of Quantum Theory* (Publications of Scuola Normale Superiore, 2011).
- [48] S. L. Braunstein and C. M. Caves, Phys. Rev. Lett. **72**, 3439 (1994).
- [49] G. C. Wick, A. S. Wightman, and E. P. Wigner, Phys. Rev. **88**, 101 (1952).
- [50] S. D. Bartlett, T. Rudolph, and R. W. Spekkens, Reviews of Modern Physics **79**, 555 (2007).
- [51] P. Hyllus, L. Pezzé, and A. Smerzi, Phys. Rev. Lett. **105**, 120501 (2010).
- [52] J. Chwedeńczuk, L. Pezzé, F. Piazza, and A. Smerzi, Phys. Rev. A **82**, 032104 (2010).